Generic First Order Orientation Transition of Vortex Lattices in Type II Superconductors

Kenta M. Suzuki, Kenji Inoue, Predrag Miranović[1], Masanori Ichioka, and Kazushige Machida

Department of Physics, Okayama University, Okayama 700-8530
[1]*Department of Physics, University of Montenegro, 81000 Podgorica, Montenegro*

First order transition of vortex lattices (VL) observed in various superconductors with four-fold symmetry is explained microscopically by quasi-classical Eilenberger theory combined with non-local London theory. This transition is intrinsic in the generic successive VL phase transition due to either gap or Fermi velocity anisotropies. This is also suggested by the electronic states around vortices. Ultimate origin of this phenomenon is attributed to some what hidden frustrations of a spontaneous symmetry broken hexagonal VL on the underlying four-fold crystalline symmetry.

KEYWORDS: vortex lattice transition, anisotropic superconductors, Eilenberger theory, non-local London theory

Morphology of vortex lattices (VL) in the Shubnikov (mixed) state of type II superconductors is not completely understood microscopically.[1,2] Thorough understanding of the VL symmetries and its orientation with respect to the underlying crystalline lattice are important both from the fundamental physics point of view because through those studies we can obtain the information on pairing symmetry (see below). It is also important from technological application of a superconductor, such as vortex pinning mechanism which ultimately determines critical current density.

The first neutron diffraction experiment[3] was conducted for Nb to observe a periodic array of the Abrikosov vortices. Concurrently since then various experimental methods have been developed, such as Bitter decoration of magnetic fine particles, μSR, NMR or scanning tunneling microscope (STM).[1,2] The former ones are to observe spatial distribution of the magnetic field in VL and the last one is to observe the electronic structure of VL. The variety of experiments compile a large amount of information on VL morphology. Thus we need to synthesize many fragmented pieces of information which has been not done yet. Here we are going to investigate a mystery known for a quite some time and to demonstrate that the present methodology is powerful enough which might be useful for systematic studies of Shubnikov state in type II superconductors.

As shown in Fig. 1 where the open angle θ of a unit cell is plotted as a function of magnetic field B applied to the four-fold symmetric axis (001) in either cubic crystal (V_3Si[4,5]) or tetragonal crystals (YNi_2B_2C,[6–8] $CeCoIn_5$[9]), the observed VL symmetries change in common, yet they belong to completely different superconducting classes (conventional or unconventional): Namely starting with the regular triangle lattice at the lower critical field B_{c1}, the VL transforms into a general hexagonal lattice with $\theta \neq 60°$, keeping the orientation $\boldsymbol{a}$ the same: parallel to (110). This direction is defined as (110) here, so that $\boldsymbol{a} \parallel$ (110). The inset of Fig. 1 shows
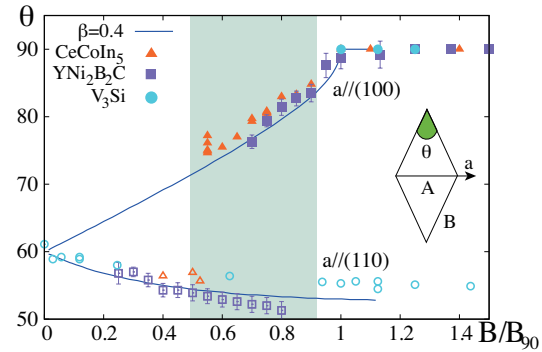

Fig. 1. (Color online) Field dependence of open angle θ for V_3Si ($\bigcirc$),[4,5] YNi_2B_2C ($\square$)[6–8] and $CeCoIn_5$ ($\triangle$).[9] The open and filled symbols, respectively, belong to orientation $\boldsymbol{a} \parallel$ (110) and $\boldsymbol{a} \parallel$ (100). The shaded band indicates first order transition region for these materials. Lines are theoretical curves by non-local London theory with $\beta = 0.4$ for guide of eyes. Inset shows a unit cell of VL with definitions of open angle θ, orientation direction $\boldsymbol{a}$, and bonds A and B of VL.

the definition of θ and the orientation $\boldsymbol{a}$. At a certain field B_{1st} (shaded area in Fig. 1) whose values depends in external conditions, such as cooling rate, etc., the orientation $\boldsymbol{a}$ suddenly changes by angle 45° to $\boldsymbol{a} \parallel$ (100) at a first order phase transition. Upon further increasing B, θ continuously increases and finally becomes $\theta = 90°$ at B_{90}. This lock-in transition at $B = B_{90}$ is of second order. Those successive symmetry changes in VL are common for those compounds. Other A-15 compounds Nb_3Sn[10] or $TmNi_2B_2C$[11] exhibit a similar trend.

We explain this phenomenon by synthesizing two theoretical frameworks: phenomenological non-local London theory[12–14] and microscopic Eilerberger theory.[15–17] The purpose of this study is to examine the universal behaviors of first order transition in the VL morphology under changing the degree of anisotropies coming from two sources: the Fermi velocity anisotropy and superconducting gap anisotropy. In this analysis, we evaluate

the validity of non-local London theory, comparing with quantitative estimates by Eilenberger theory. Further, we discuss intrinsic reasons why the first order transition of VL orientation occurs, in viewpoints from frustrations and electronic states around vortices. Microscopic calculation is necessary to discuss the electronic states.

As we will see below, frustrations are a crucial key concept to understand this phenomenon. Antiferromagnetic spins on a triangular lattice is a well known example of frustration. Here a triangular VL is also a driving force due to hidden frustration which is more subtle than the spin case, leading to successive phase transition. Hexagonal symmetry is incompatible with four-fold symmetry of underlying crystal lattice, because all bonds between vortices are not satisfied simultaneously to lower bonding energies.

Quasi-classical Eilenberger theory[15–17] is valid for $k_F\xi \gg 1$ (k_F: the Fermi wave number and ξ: the coherence length) a condition met in the superconductors of interest here. Eilenberger equations read as

$$(\omega_n + \boldsymbol{v}(\theta) \cdot (\boldsymbol{\Pi} + i\boldsymbol{A})) f = \Delta(\boldsymbol{r},\theta)g, \qquad (1)$$

$$(\omega_n - \boldsymbol{v}(\theta) \cdot (\boldsymbol{\Pi} - i\mathbf{A})) f^\dagger = \Delta^*(\boldsymbol{r},\theta)g \qquad (2)$$

with $g^2 + ff^\dagger = 1$ for quasi-classical Green's functions $g(\omega_n,\boldsymbol{r},\theta)$, $f(\omega_n,\boldsymbol{r},\theta)$, and $f^\dagger(\omega_n,\boldsymbol{r},\theta)$. In our formulation, we use Eilenberger unit where length, magnetic field and temperature are, respectively, scaled by $R_0 = \hbar v_{F0}/2\pi k_B T_c$, $B = \phi_0/2\pi R_0^2$, and transition temperature T_c with flux quantum ϕ_0. Matsubara frequency $\omega_n = T(2n+1)$ with integer n. The pairing interaction is assumed separable $V(\theta,\theta') = V_0\phi(\theta)\phi(\theta')$ so that gap function is $\Delta(\boldsymbol{r},\theta) = \Psi(\boldsymbol{r})\phi(\theta)$. Since we consider two-dimensional case with cylindrical Fermi surface, we set the normalized Fermi velocity $\boldsymbol{v}(\theta) \equiv \boldsymbol{v}_F/v_{F0}$ as $\boldsymbol{v}(\theta) = v(\theta)(\cos\theta, \sin\theta)$. When we discuss the Fermi velocity anisotropy, we model it as $v(\theta) = (1+\beta\cos4\theta)/\sqrt{1-\beta^2}$ and $\phi(\theta) = 1$, which is called β model.[17] When we discuss the gap anisotropy, $v(\theta) = 1$ and $\phi(\theta)^2 = 1-\alpha\cos4\theta$ as α-model (anisotropic s-wave), or $\phi(\theta) = \sqrt{2}\cos2\theta$ as d-wave pairing. Here θ is the polar angle relative to (100) axis.

The selfconsistent equations for the gap function $\Psi(\boldsymbol{r})$ and vector-potential $\boldsymbol{A}(\boldsymbol{r})$ are

$$\Psi(\boldsymbol{r}) = V_0 N_0\, 2T \sum_{\omega_n > 0} \langle \phi^*(\theta)f \rangle \qquad (3)$$

$$\boldsymbol{\nabla} \times \boldsymbol{\nabla} \times \boldsymbol{A}(\boldsymbol{r}) = -\frac{2T}{\kappa^2} \sum_{\omega_n > 0} \mathrm{Im}\,\langle \boldsymbol{v}g \rangle. \qquad (4)$$

with $V_0 N_0 = \ln T + 2T \sum_{\omega_n>0} \omega_n^{-1}$ and Ginzburg Landau parameter κ. For average over Fermi surface, $\langle\ldots\rangle = \int_0^{2\pi}(\ldots)d\theta/2\pi v(\theta)$ with extra factor $1/v(\theta)$ coming from angle-resolved density of states $N(\theta) = N_0/v(\theta)$ on Fermi surface. The self-consistent solution yields a complete set of the physical quantities: the spatial profiles of the order parameter $\Psi(\boldsymbol{r})$ and the magnetic field $B(\boldsymbol{r})$. The local density of sates (LDOS) for electronic states is calculated by $N(\boldsymbol{r},E) = N_0\mathrm{Re}\langle g(\omega_n,\boldsymbol{r},\theta)|_{i\omega_n\to E+i0}\rangle$.

The free energy density is given by

$$F = \kappa^2\overline{B^2(\boldsymbol{r})} - T\sum_{\omega_n>0} \overline{\left\langle \frac{1-g}{1+g}(\Delta^*f + \Delta f^\dagger) \right\rangle}.$$

Here, $\overline{(\ldots)}$ is a spatial average within a unit cell of VL. Free energy should be minimized with respect to the VL symmetry and its orientation relative to the crystallographic axes. In previous studies by Eilenberger theory, the first order transition of the VL orientation was not evaluated at low T, while only the transition from triangular to square VL was discussed.[16, 17] In principle, we can investigate the whole space spanned by (B, T). But in practice it is not easy to exhaust the parameters in order to seek the desired physics. Thus our calculations are backed up by the non-local London theory.

The non-local London theory is powerful and handy for $B_{c1} \lesssim B$ at low T. The nonlocal relation between current $\boldsymbol{j}$ and vector potential $\boldsymbol{A}$ in Fourier space is derived as $\frac{4\pi}{c}j_l(\boldsymbol{q}) = i[\boldsymbol{q} \times \boldsymbol{A}]_l = -\kappa^{-2}\sum_m Q_{lm}(\boldsymbol{q})A_m(\boldsymbol{q})$ ($l, m = x, y$) from the Eilenberger theory.[13] Since we use the Eilenberger unit here, the penetration depth λ is changed to κ in the length unit R_0 ($\sim \xi$). The kernel is

$$Q_{lm}(\boldsymbol{q}) = 2T \sum_{\omega_n>0} \left\langle \frac{|\Delta(\theta)|^2 v_l v_m}{\beta_n(\beta_n^2 + (\boldsymbol{v} \cdot \boldsymbol{q})^2)} \right\rangle \qquad (5)$$

with $\beta_n^2 = \omega_n^2 + \Delta^2(\theta)$, and $\Delta(\theta)$ is a uniform solution of the gap function. In previous studies by the non-local London theory for the first order transition in borocarbides, higher order terms than q^4 was neglected.[12] Here, we do not expand Q_{lm} by q so that we can include all order contributions of q in Q_{lm}.[14] The corresponding London free energy is given by

$$F_L = \sum_{\boldsymbol{q}} e^{-\frac{1}{2}\xi^2 q^2}[1 + \kappa^2\{(Q^{-1})_{yy}q_x^2$$
$$+ (Q^{-1})_{xx}q_y^2 - 2(Q^{-1})_{xy}q_x q_y\}]^{-1}, \quad (6)$$

where Q^{-1} is the inverse matrix of Q_{lm} depending on $\boldsymbol{q}$. The non-local London theory is valid near B_{c1} at lower T where the vortex core contribution is approximated as a cutoff parameter ξ mimicking the finite core size effect. To explore wide ranges of (B, T) on a firm basis, we need to carefully check the validity of non-local London theory, using Eilenberger theory. We report our results for $\kappa = 89$ and $T = 0.2T_c$ in both theories. The results do not depend on the κ value unless κ is approaching $1/\sqrt{2}$.

First, we study the β-model, i.e., anisotropy of Fermi velocity. Figure 2 shows a stereographic view of the open angle θ as functions of B and β. It is seen that (1) irrespective of the β values the first order transition exists seen as a jump of θ in Fig. 2. (2) The jump of the first order transition becomes large as β increases. (3) $\beta > \beta_{cr} = 0.38$ ($\beta < \beta_{cr}$) at $T/T_c = 0.2$, the square lattice is (never) realized. (4) This square lattice becomes ultimately unstable for higher fields. Items (3) and (4) were also confirmed by Eilenberger calculation [see Fig. 2(a) in Ref. 17]. Note in passing that in CeCoIn$_5$ the square lattice changes into a hexagonal lattice at a higher field, which reminds us the similarity, but we believe that
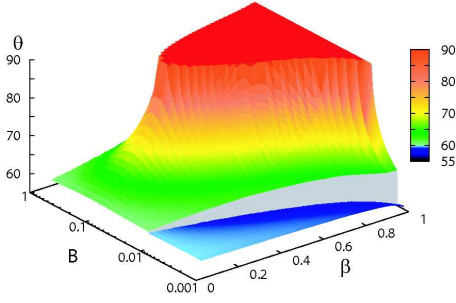
Fig. 2. (Color online) Stereographic view of the open angle θ as functions of B and β in the β-model by non-local London theory. First order transitions from $\theta < 60°$ to $\theta > 60°$ with $45°$ rotation of VL orientation are seen for any values of β.

Fig. 4. (Color online) Zero energy LDOS $N(\boldsymbol{r}, E = 0)/N_0$ for hexagonal VL with $\theta \sim 60°$ at $B/B_{90} = 0.07$ in $d_{x^2-y^2}$-wave pairing, where the gap minimum is along (110) direction. (a) Stable orientation $\boldsymbol{a} \parallel$ (110). (b) Unstable orientation $\boldsymbol{a} \parallel$ (100). Horizontal axis is parallel to $\boldsymbol{a}$-direction.
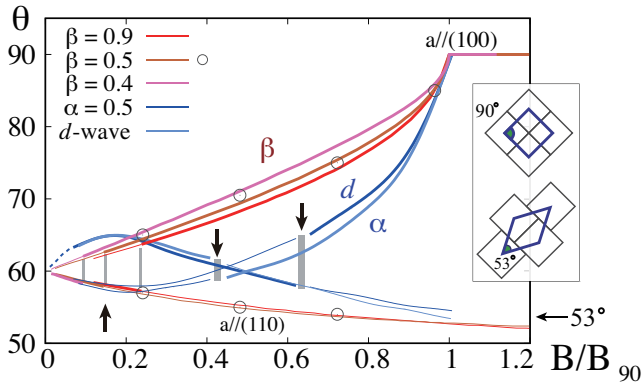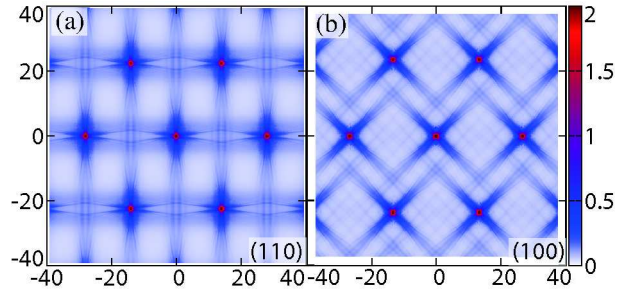

Fig. 3. (Color online) Open angle θ as a function of B/B_{90} for two orientations in the β-model ($\beta = 0.4, 0.5, 0.9$) by non-Local London, and in the α-model ($\alpha = 0.5$) and d-wave model by Eilenberger theory. Circles show θ obtained by Eilenberger theory in the β-model with $\beta = 0.5$. Arrows indicate B_{1st}. Inset shows the closed packed square tiles and the associated hexagonal unit cell, indicating $\theta = 53°$ (lower inset) and $\theta = 90°$ (upper inset) when $B \to B_{90}$.
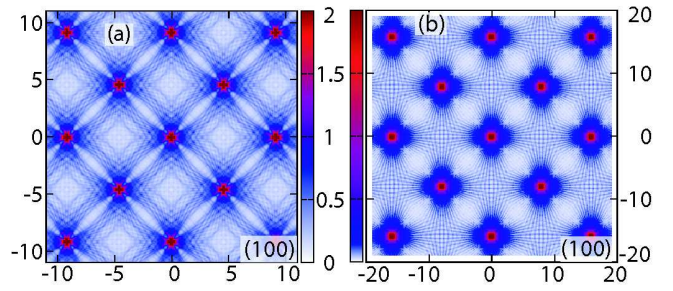

Fig. 5. (Color online) Zero energy LDOS $N(\boldsymbol{r}, E = 0)/N_0$ for the square VL with $\boldsymbol{a} \parallel$ (100) at $B/B_{90} = 1.2$ in the $d_{x^2-y^2}$-wave case (a) and the β-model with $\beta = 0.5$ (b).

it is caused by other effect, such as the Pauli paramagnetic effect.[19, 20]

When plotted as a function of B/B_{90} by respective lock-in field B_{90} as shown in Fig. 3, the θ-behaviors are similar for any β ($> \beta_{cr}$), while B_{1st} changes depending on β. These universal behaviors well reproduce the experimental data as shown in Fig. 1. We also plot some points of θ obtained by Eilenberger theory for $\beta = 0.5$ (see the circle symbols in Fig. 3), which shows similar behavior as in the non-local London theory. Therefore, the non-local London theory can be applied reliably to superconductors whose anisotropy comes from the Fermi velocity.

Next, we study the case of anisotropic pairing gap by the α-model and d-wave pairing. Figure 3 also shows θ-behavior in these cases obtained by Eilenberger theory. Even in the gap anisotropy, we find the first order transition of orientation, where the θ-dependence is not monotonic at low B and B_{1st} is higher compared to the β-model. Thus, independent of the sources of anisotropy (Fermi velocity or gap), there is always the first order orientational transition in the similar successive VL transition. Starting with $\theta = 60°$ at B_{c1}, the $\boldsymbol{a}$-direction of

VL coincides with the gap minimum (α-model) or with the Fermi velocity minimum (β-model). This orientation is changed via a first order transition to the orientation where the $\boldsymbol{a}$-direction is rotated by $45°$. However, in the gap anisotropy case, the reentrant transition from square to hexagonal VL at high fields does not occur. We note that in these anisotropic gap cases, at low T the non-local theory does not work to reproduce the θ-behaviors of Eilenberger calculation.[14]

It is also interesting to notice simple geometry that the open angle $\theta_{\min} = 2\tan^{-1}(\frac{1}{2}) = 53°$ when square tiles with same size are closely packed as shown in lower inset of Fig. 3. In the VL orientation $\boldsymbol{a} \parallel$ (110), as seen from Fig. 3, the theoretical minimum of θ indicates $\theta_{\min} \sim 53°$ for both anisotropy cases, which is roughly obeyed by the experimental data shown in Fig. 1. In the other orientation $\boldsymbol{a} \parallel$ (100), $\theta \to 90°$ at $B \to B_{90}$. This is also understandable by the packing of square tiles in different way, as shown in upper inset of Fig. 3.

It is instructive to examine the electronic structures of various VL's to understand the origins of the successive transition. First, we discuss stable orientation of hexagonal VL at low B in the $d_{x^2-y^2}$-wave pairing. In Fig. 4 we display the typical LDOS at zero energy (i.e., Fermi level) for two orientations. In stable orientation $\boldsymbol{a} \parallel$ (110) in (a), the zero energy LDOS is well connected between nearest neighbor (NN) vortices along $\boldsymbol{a}$, and between next NN vortices. Here $\boldsymbol{a}$ is parallel to node direction of d-wave pairing, connected by the A-type bond in inset of Fig. 1. These interconnections effectively lower the

kinetic energy of quasi-particles, leading to a stable VL symmetry and orientation. In contrast, in the VL of unstable orientation in (b), the interconnections are not well organized, clearly demonstrating it less favorable orientation and VL symmetry energetically. We note that, even in the stable hexagonal VL [Fig. 4(a)], four B type bonds defined in inset of Fig. 1 among the six NN vortex bonds are not favorable directions for interconnections. Thus those are frustrated, which ultimately leads to further successive VL transitions in higher fields.

The concept of interconnections between NN vortices via zero energy LDOS continues to be useful for square VL at high fields. In d-wave pairing as shown in Fig. 5(a), interconnections are highly well organized to stabilize it. In particular not only all NN vortex connections are tightly bound, but also second, third neighbor vortices are also connected. This high field stable VL configuration can not be continuously transformed from low field stable hexagonal VL in Fig. 4(a)just by changing θ. Therefore there must exist a first order phase transition in an intermediate field region to rotate the orientation by $45°$. This intuitive explanation is basically correct for a superconductor with the four-fold anisotropy coming from the Fermi velocity anisotropy.

In the β-model shown in Fig. 5(b) in the stable square VL, the zero energy LDOS extends broadly to neighbor vortices. This weak connection between vortices ultimately leads to the instability for this square VL in the β-model towards a hexagonal VL in higher fields as shown in Fig. 2. This may be one of the reasons for the reentrance phenomenon in the β-model. Note that in the α-model there is no reentrance up to B_{c2} and the square VL is most stable at high fields.

Let us examine the experimental data in light of the present calculations. V_3Si[4,5] whose data are shown by circle symbols in Fig. 1 and Nb_3Sn[10] are cubic crystals with A-15 structure and known to be an s-wave superconductor with an isotropic gap. The main four-fold anisotropy comes from the Fermi velocity, thus an example of the β-model. YNi_2B_2C[6–8] (the squares in Fig.1) has tetragonal crystal and is known to be d_{xy}-like gap symmetry,[18] thus an example of the α-model albeit the Fermi velocity anisotropy may be also working. In fact, the successive transition precisely follows our calculation, ending up with the square VL whose NN is directed to (100).[6–8] There is no indication for the reentrance transition up to B_{c2}. $CeCoIn_5$[9] (the triangles in Fig.1) has a $d_{x^2-y^2}$ gap symmetry. The successive transition, including first order, ends up with the square VL which orients along (110) as expected. Towards B_{c2} it exhibits the reentrant transitions to the hexagonal VL with the same orientation near B_{c1}. Similar reentrant VL transition is also found in $TmNi_2B_2C$.[11] This intriguing reentrance phenomenon, which is not covered here, belonging to a future problem because we need to consider the Pauli paramagnetic effect.[19,20]

In conclusion, universal behaviors of the first order transition in the VL morphology from hexagonal to square lattice have been studied by the non-local London theory and Eilenberger theory. We find that non-local London theory is accurate for the superconductor whose anisotropy comes from the Fermi velocity, while it is uncontrollable for the gap anisotropy case, which is covered by Eilenberger theory. We have explained the successive VL transition with first order one observed in various four-fold symmetric superconductors. Since the origin of this phenomenon is due to either gap anisotropy or Fermi velocity anisotropy, which are present in any superconductors, it is desirable to carefully perform experiments of neutron diffraction, μSR, NMR or STM to observe this generic phenomenon. In particular it is interesting to see it in high T_c cuprates, Sr_2RuO_4 and $TmNi_2B_2C$ for $H//(001)$, which are known to have four-fold gap anisotropy, yet so far this phenomenon has not been reported although square VL's are observed.

1) *Anisotropy Effects in Superconductors*, edited by H. Weber (Plenum, New York, 1977).
2) H.E. Brandt: Rep. Prog. Phys. **58** (1995) 1465.
3) D. Cribier, B. Jacrot, L. M. Rao, and B. Farnoux: Phys. Lett. **9** (1964) 106.
4) M. Yethiraj, D.K. Christen, A.A. Gapud, D.McK. Paul, S.J. Crowe, C.D. Dewhurst, R. Cubitt, L. Porcar, and A. Gurevich: Phys. Rev. B **72** (2005) 060504(R).
5) C.E. Sosolik, J.A. Stroscio, M.D. Stiles, E.W. Hudson, S.R. Blankenship, A.P. Fein, and R.J. Celotta: Phys. Rev. B**68** (2003) 140503(R).
6) S.J. Levett, C.D. Dewhurst, and D.McK. Paul: Phys. Rev. B **66** (2002) 014515.
7) C.D. Dewhurst, S.J. Levett, and D.McK. Paul: Phys. Rev. B **72** (2005) 014542.
8) D.McK. Paul, C.V. Tomy, C.M. Aegerter, R. Cubitt, S.H. Lloyd, E.M. Forgan, S.L. Lee, and M. Yethiraj: Phys. Rev. Lett. **80** (1998) 1517.
9) A.D. Bianchi, M. Kenzelmann, L. DeBeer-Schmitt, J.S. White, E.M. Forgan, J. Mesot, M. Zolliker, J. Kohlbrecher, R. Movshovich, E.D. Bauer, J.L. Sarrao, Z. Fisk, C. Petrovic, and M.R. Eskildsen: Science **319** (2008) 177.
10) R. Kadono, K.H. Satoh, A. Koda, T. Nagata, H. Kawano-Furukawa, J. Suzuki, M. Matsuda, K. Ohishi, W. Higemoto, S. Kuroiwa, H. Takagiwa, and J. Akimitsu: Phys. Rev. B **74** (2006) 024513.
11) M.R. Eskildsen, K. Harada, P.L. Gammel, A.B. Abrahamsen, N.H. Andersen, G. Ernst, A.P. Ramirez, D.J. Bishop, K. Mortensen, D.G. Naugle, K.D.D. Rathnayaka, and P.C. Canfield: Nature **393** (1998) 242.
12) V.G. Kogan, P. Miranović, L. Dobrosavljević-Grujić, W.E. Pickett, and D.K. Christen: Phys. Rev. Lett. **79** (1997) 741; V.G. Kogan, M. Bullock, B. Harmon, P. Miranović, L. Dobrosavljević-Grujić, P.L. Gammel and D.J. Bishop: Phys. Rev. B **55** (1997) R8693.
13) V.G. Kogan, A. Gurevich, J.H. Cho, D.C. Johnston, M. Xu, J.R. Thompson, and A. Martynovich: Phys. Rev. B **54** (1996) 12386.
14) M. Franz, I. Affleck, and M.H.S. Amin: Phys. Rev. Lett. **79** (1997) 1555.
15) G. Eilenberger: Z. Phys. **214** (1968) 195.
16) M. Ichioka, A. Hasegawa and K. Machida: Phys. Rev. B**59** (1999) 184 and 8902.
17) N. Nakai, P. Miranović, M. Ichioka, and K. Machida: Phys. Rev. Lett. **89** (2002) 237004.
18) H. Nishimori, K. Uchiyama, S. Kaneko, A. Tokura, H. Takeya, K. Hirata and N. Nishida: J. Phys. Soc. Jpn. **73** (2004) 3247.
19) N. Hiasa and R. Ikeda: Phys. Rev. Lett. **101** (2008) 027001.
20) K.M. Suzuki, M. Ichioka, and K. Machida: Proc. M^{2}S-IX, Tokyo (2009).